A Water Cherenkov Test Beam Experiment for Hyper-Kamiokande and Future Large-scale Water-based Detectors

M. Barbi and N. Kolev
University of Regina, Department of Physics, Regina, Saskatchewan, Canada

V. Berardi and M.G. Catanesi
INFN Sezione di Bari and Università e Politecnico di Bari, Dipartimento Interuniversitario di Fisica, Bari, Italy

S. Bhadra and G. Santucci
York University, Department of Physics and Astronomy, Toronto, Ontario, Canada

S. Boyd and B. Richards
University of Warwick, Department of Physics, Coventry, United Kingdom

A. Bubak, J. Holeczek, J. Kisiel, and K. Porwit
University of Silesia, Institute of Physics, Katowice, Poland

A. Buchowicz, G. Galinski, R. Kurjata, J. Marzec, W. Obrebski, G. Pastuszak, A. Rychter, K. Zaremba, and M. Ziembicki
Warsaw University of Technology, Institute of Radioelectronics and Multimedia Technology, Warsaw, Poland

M. Buizza Avanzini, O. Drapier, M. Gonin, T. Mueller, and P. Paganini
Ecole Polytechnique, IN2P3-CNRS, Laboratoire Leprince-Ringuet, Palaiseau, France

J. Cederkall
Lund University, Department of Physics, Lund, Sweden

J. Coleman, N. McCauley, C. Metelko, and Y. Schnellbach
University of Liverpool, Department of Physics, Liverpool, United Kingdom

G. Collazuol, A. Longhin, and M. Mezzetto
INFN Sezione di Padova and Università di Padova, Dipartimento di Fisica, Padova, Italy

S. Cuen-Rochin, P. de Perio, A. Konaka, T. Lindner, M. Pavin, and N. Prouse
TRIUMF, Vancouver, British Columbia, Canada

T. Dealtry, A.J. Finch, L.L. Kormos, and H.M. O'Keeffe
Lancaster University, Physics Department, Lancaster, United Kingdom

G. De Rosa, C. Riccio, and A.C. Ruggeri
INFN Sezione di Napoli and Università di Napoli, Dipartimento di Fisica, Napoli, Italy

F. Di Lodovico, T. Katori, J. Wilson, and S. Zsoldos
King's College London, Department of Physics, Strand, London WC2R 2LS, United Kingdom

P. Dunne, P. Jonsson, K. Long, M. Scott, Y. Uchida, A. Waldron, and M. Wascko
Imperial College London, Department of Physics, London, United Kingdom

T. Ekelof and E. O'Sullivan
Uppsala University, Department of Physics and Astronomy, Uppsala, Sweden

C. Giganti and M. Guigue
Sorbonne Université, Université Paris Diderot, CNRS/IN2P3, Laboratoire de Physique Nucléaire et de Hautes Energies (LPNHE), Paris, France

R. Gornea
Carleton University, Department of Physics, Ottawa, Canada and TRIUMF, Vancouver, British Columbia, Canada

CERN-SPSC-2019-042 / SPSC-I-254
07/10/2019

M. Hartz
TRIUMF, Vancouver, British Columbia, Canada and
Kavli Institute for the Physics and Mathematics of the Universe (WPI), The University of Tokyo Institutes for Advanced Study, University of Tokyo, Kashiwa, Chiba, Japan

A. Ioannisyan
Yerevan Physics Institute, Yerevan, Armenia

T. Ishida and T. Nakadaira
High Energy Accelerator Research Organization (KEK), Tsukuba, Ibaraki, Japan

M. Ishitsuka and M. Shinoki
Tokyo University of Science, Faculty of Science and Technology, Department of Physics, Noda, Chiba, Japan

B. Jamieson and J. Walker
University of Winnipeg, Department of Physics, Winnipeg, Manitoba, Canada

D. Karlen
University of Victoria, Department of Physics and Astronomy, Victoria, British Columbia, Canada and TRIUMF, Vancouver, British Columbia, Canada

U. Katz, J. Reubelt, and C. van Eldik
Friedrich Alexander University Erlangen-Nurnberg, Department of Physics, Erlangen, Germany

A. Khotjantsev, Y. Kudenko, A. Shaykina, S. Suvorov, and N. Yershov
Institute for Nuclear Research of the Russian Academy of Sciences, Moscow, Russia

K. Kowalik, J. Lagoda, P. Mijakowski, E. Rondio, J. Zalipska, and G. Zarnecki
National Centre for Nuclear Research, Warsaw, Poland

M. Kuze
Tokyo Institute of Technology, Department of Physics, Tokyo, Japan

L. Ludovici
INFN Sezione di Roma and Università di Roma "La Sapienza", Roma, Italy

G. Nieradka and M. Suchenek
Nicolaus Copernicus Astronomical Centre, Polish Academy of Sciences, Warsaw, Poland

M. Ostrowski, L. Stawarz, and K. Zietara
Jagiellonian University, Astronomical Observatory, Cracow, Poland

M. Posiadala-Zezula
University of Warsaw, Faculty of Physics, Warsaw, Poland

B. Quilain
Kavli Institute for the Physics and Mathematics of the Universe (WPI), The University of Tokyo Institutes for Advanced Study, University of Tokyo, Kashiwa, Chiba, Japan and Ecole Polytechnique, IN2P3-CNRS, Laboratoire Leprince-Ringuet, Palaiseau, France

P.J. Rajda and K. Stopa
AGH University of Science and Technology, Faculty of Computer Science, Electronics and Telecommunications, Cracow, Poland

C. Rott
Sungkyunkwan University, Department of Physics, Suwon, Korea

S.H. Seo
Center for Underground Physics, Institute for Basic Science, Daejeon, Korea

C. Vilela and M.J. Wilking
State University of New York at Stony Brook, Department of Physics and Astronomy, Stony Brook, New York, U.S.A.

CONTENTS

I. EXECUTIVE SUMMARY

Water Cherenkov and water-based particle detector technologies are used to realize multi-kiloton scale experiments such as the currently operating Super-Kamiokande experiment, the planned Hyper-Kamiokande experiment and the proposed THEIA detector and ESSnuSB detectors. These experiments are operated or proposed to study a broad range of physics including neutrino oscillations, nucleon decay, dark matter and neutrinoless double beta decay. The neutrino oscillations program will also include kiloton scale near or intermediate detectors used to study neutrino production and interactions in the absence of neutrino oscillations, such as the Hyper-K Intermediate Water Cherenkov Detector (IWCD). Realization of these physics programs will require new detector technologies and percent level calibration of detector responses and models of physics processes within the detector. Here we describe our intent to propose a 50 ton scale Water Cherenkov test experiment (WCTE) to be deployed in a North or East test beam experimental area. The experiment will include a secondary target located just upstream of the experiment in order to produce very low energy particle fluxes, including charged pions. The WCTE program will be carried out with the following objectives:

- Operate and understand the performance of new detector technologies such as multi-PMTs, dichroicon wavelength-separating cones and water-based liquid scintillator in a fully integrated detector.
- Study the performance of a < 1 kiloton scale water Cherenkov detector with known particle fluxes, and test and develop calibration systems necessary for accurate modeling of a detector of this size.
- Measure important physics processes for the modeling of water Cherenkov detector responses, including high-angle Cherenkov light production, pion scattering and absorption, and secondary neutron production in hadron scattering.

We aim to start operation of the water Cherenkov test experiment in 2021-2022.

II. INTRODUCTION & MOTIVATION

Water Cherenkov detectors have long been used in experiments measuring or searching for low rate processes such as neutrino interactions or proton decay. A significant appeal of the technology is the capability to scale it to large detector masses of multiple kilotons. The currently operating Super-Kamiokande (Super-K) detector and proposed detectors such as Hyper-Kamiokande (Hyper-K), THEIA and the ESSnuSB detector will advance the water Cherenkov technology by adding new detection capabilities and by entering a regime of precision measurements not previously explored for GeV scale neutrino events.

The Super-K collaboration plans to load $Gd_2(SO_4)_3$ into the Super-K detector for enhanced neutron detection capability with captures on Gd. The neutron detection capability will expand the physics program with the ability to tag inverse β decay events, antineutrino interactions and atmospheric neutrino backgrounds for proton decay searches.

Hyper-K will make neutrino oscillation measurements with unprecedented precision, requiring 1% level control of systematic uncertainties. For this purpose, a new 1 kiloton scale Intermediate Water Cherenkov Detector (IWCD) is proposed to make precision neutrino rate measurements. The IWCD will utilize new high resolution photosensors in order to achieve the necessary performance for GeV scale neutrino interactions in a detector of < 10 m in size. The Hyper-K experiment plans to use neutron tagging in measurements such at the supernova relic neutrino search or nucleon decay searches. Hyper-K, will be sensitive to uncertainties on neutron production in a manner similar to Super-K.

The THEIA experiment will deploy water-based liquid scintillator (WbLS) to increase the light output compared to a typical water Cherenkov detector and to add sensitivity to charged particles below the Cherenkov threshold. In order to detect and separate the directional Cherenkov light and isotropic scintillation light, new photosensor technologies are being developed that take advantage of the differing time and spectral distributions of Cherenkov and scintillation light.

The advancements in detection technology for water Cherenkov detectors listed above require extensive R&D programs that should include deployment of the prototype technologies in a test beam experiment with known particle energies and types entering the detector. Here, we express our intent to propose a water Cherenkov test experiment (WCTE) in the CERN North Area or East Area. Additional details of the motivation for the WCTE and details of the WCTE itself are provided in the following sections.

A. Hyper-Kamiokande Experiment and IWCD

Hyper-Kamiokande (Hyper-K) is a next-generation particle physics experiment with a broad physics program including neutrino oscillation measurements, nucleon decay searches, supernova burst and relic neutrino detection, and dark matter searches [1]. The Hyper-K detector is a 260 kiloton water Cherenkov detector. For the long baseline neutrino oscillation program, the Hyper-K detector will be used to study the oscillations of neutrinos produced at the J-PARC accelerator in Tokai, Japan. The core of the neutrino oscillation measurement program is the search for CP violation in the oscillation channels $\nu_\mu \rightarrow \nu_e$ and $\bar{\nu}_\mu \rightarrow \bar{\nu}_e$. Hyper-K will collect approximately 2000 candidate events in each of these oscillation modes after 10 years of operation, allowing for a measurement of the CP asymmetry with 3% statistical uncertainty. To take full advantage of the statistical power of the experiment, individual sources of systematic uncertainty must be controlled to the 1% level or better. Dominant sources of systematic uncertainty arise in the modeling of neutrino production, neutrino interactions and the detector responses.

To control systematic uncertainties related to neutrino production and interaction modeling, the Hyper-K collaboration has proposed a suite of near detectors to study the neutrinos at short baselines before the oscillation effect is significant. This suite includes the Intermediate Water Cherenkov Detector (IWCD), based off of the design of the previously proposed NuPRISM detector [2]. The IWCD, illustrated in Fig. 1, is a 10 m diameter by 8 m tall water Cherenkov detector deployed in a 50 m deep pit about 1 km from the J-PARC neutrino source. The detector's elevation in the pit

can be varied by controlling the water level of the pit, allowing measurements to be made at varying angles relative to the average neutrino direction, probing different neutrino energies. The detector includes a 1 m thick optically separated veto region at the outer edge of the detector volume, leaving an 8 m diameter by 6 m tall region for physics measurements. The IWCD will be instrumented with newly developed multi-photomultipier tube (mPMT) photosensors with improved timing and spatial resolution to enable the event reconstruction performance necessary for a detector of this size.

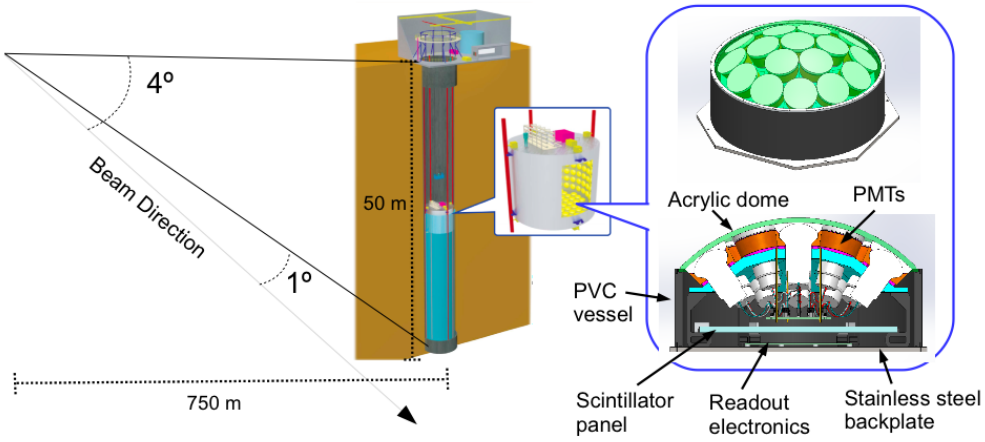

FIG. 1. Schematic overview of the IWCD.

The IWCD physics program will include three important measurements described here. Since Hyper-K will search for CP violation in the channels $\nu_\mu \rightarrow \nu_e$ and $\bar{\nu}_\mu \rightarrow \bar{\nu}_e$, it is necessary to measure the interaction cross section ratios $\sigma(\nu_e)/\sigma(\nu_\mu)$ and $\sigma(\bar{\nu}_e)/\sigma(\bar{\nu}_\mu)$ with precision of 3-4% or better. This measurement requires controlling relative uncertainties on the modeling of the detector response to $\nu_e(\bar{\nu}_e)$ and $\nu_\mu(\bar{\nu}_\mu)$ at the 2% level or better. This requires precise understanding of the event reconstruction efficiency, particle identification efficiency and vertex reconstruction, which affects the effective fiducial mass, in the candidate interactions.

The IWCD will also study the energy dependence of neutrino interactions by making measurements with the detector located at different off-axis angles, allowing the neutrino spectrum to vary. These measurements require that the detector response be maintained within 1% during operation to ensure unbiased interpretation of the off-axis angle dependence of the measurements. The measurements at different off-axis angles will be used to relate the reconstructed final state topologies and kinematic properties to the neutrino energy. Hence, correct modeling of the efficiency to detect final state particles and reconstruct their kinematic properties will be critical. For example, interpretation of the measurements at varying off-axis angles requires an energy scale uncertainty of 0.5% or less for the IWCD.

The IWCD will also be used to measure with high statistics the production of neutrons in neutrino interactions. This will be achieved by loading the detector with $Gd_2(SO_4)_3$ to enhance the neutron capture cross section and increase the efficiency to reconstruct neutron capture events. These measurements will be used as inputs to Super-K and Hyper-K neutrino and nucleon decay analyses that use neutron multiplicity measurements to identify signal or background events. The interpretation of the IWCD neutron multiplicity data will require an understanding of the secondary neutrons produced when various final state particles traverse the detector medium.

To achieve the full physics sensitivity of Hyper-K and IWCD, it is necessary to calibrate the detectors and understand the detectors' responses with $\sim 1\%$ accuracy. This includes unbiased modeling of the energy scale, detection efficiency, particle identification and fiducial region in the event reconstruction. The WCTE will provide a platform to develop the percent level calibration techniques with particle fluxes of known type and kinematic properties. The WCTE will also probe important physics processes for the understanding of final state signatures, such as the production of high energy delta rays that produce Cherenkov light, the scattering and absorption of pions in the detector, and the secondary production of neutrons in the detector.

B. THEIA Detector

The proposed Theia detector would deploy Water-based Liquid Scintillator (WbLS) to allow for the simultaneous detection of both Cherenkov and scintillation light. The physics program for such a detector is broad, ranging from solar neutrino measurements and an eventual search for neutrinoless double beta decay to long-baseline neutrino physics in

the LBNF beamline and the search for nucleon decay. At low energies, the scintillation signal provides additional light collection to improve the energy resolution and identify most of the radioactive backgrounds, whereas the Cherenkov light provides direction reconstruction to improve background discrimination. At higher energies, WbLS can provide additional discrimination between various multi-particle final states by providing extra sensitivity to particles not typically seen in a traditional water-Cherenkov detector, such as low energy protons.

These potential benefits can only be realized if the additional scintillation light does not substantially degrade the reconstruction performance relative to a pure Cherenkov detector. Several experiments, such as ANNIE and WATCHMAN, are planned to study the performance of WbLS from a neutrino source, but event reconstruction outputs, such as particle identification, depend on exploiting subtle differences in the detected light patterns, and such effects are difficult to study in neutrino interactions due to uncertainties in the kinematics of final state particles from these interactions. The WCTE would provide particles of known momentum both above and below the Cherenkov threshold, which can be used to study the evolution of the Cherenkov/scintillation ratio as a function of momentum, as well as the associated reconstruction performance.

C. ESSnuSB Experiment

The ESSnuSB experiment [3, 4] proposes to use a neutrino super beam generated at the European Spallation Source (ESS) with a beam power of 5 MW and primary proton energy of 2.5 GeV. The spectrum of neutrinos produced at the ESS will have a mean energy of 0.4 GeV. At a baseline of 540 km, the neutrino spectrum is peaked at the second oscillation maximum, allowing for an enhanced measurement of the CP violation effect compared to measurements at the first oscillation maximum. A megaton scale water Cherenkov detector with a fiducial mass of 500 kilotons, based on the design of the MEMPHYS water Cherenkov detector elaborated in the earlier EU Design Studies, and shown in Fig. 2, is proposed. This detector will take advantage of improvements to photon detector performance in a similar manner as the Hyper-K detector, and will be sensitive to many of the same systematic uncertainties. The ESSnuSB experiment will also require a near detector to control systematic uncertainties on the modeling of the neutrino production and neutrino interactions. Currently the performance of a small water Cherenkov counter as part of this Near Detector is being investigated through simulations. A kiloton scale intermediate detector with the varying off-axis capability similar to the IWCD is another near detector option that may be considered. The ESSnuSB project will benefit from the WCTE as it will provide a platform to study and develop the detection technologies that are being considered for the ESSnuSB experiment.

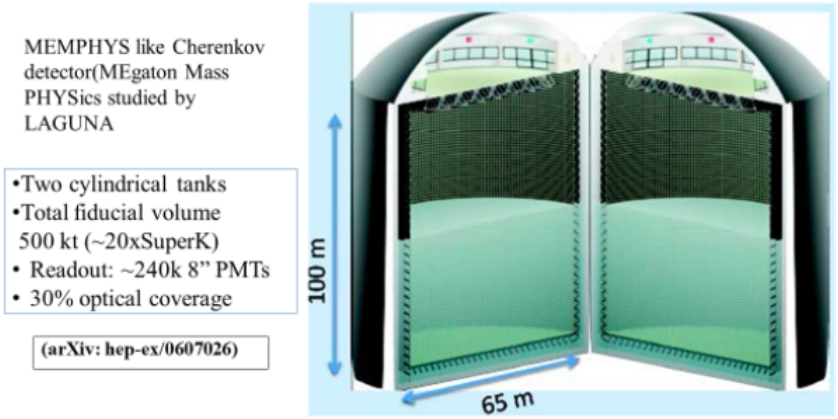

FIG. 2. Drawing of the MEMPHYS water Cherenkov detector design.

D. Water Cherenkov Test Experiment Overview

The conceptual drawing of the WCTE is shown in Fig. 3. The water tank for the detector has a diameter of ~ 3.8 m and a height of ~ 3.5 m. The goal of the experiment is to measure the properties of charged particles of type $\pi^{\pm}$, p^{+}, $e^{\pm}$, $\mu^{\pm}$ and $K^{\pm}$ with incident momenta ranging from ~ 140 MeV/c to ~ 1200 MeV/c as they traverse the detector. The configuration in Fig. 3 (top) is necessary to achieve the low momentum pion beam. The secondary target is placed close to the detector so that low momentum pions can reach the detector before decaying. This configuration requires careful design of the shielding and orientation of the spectrometer and detector so that background tertiary particles

are minimized. For incident $\mu^{\pm}$, a different beam configuration will be used with the secondary target placed further upstream to allow distance for the pions to decay. Configurations optimized for neutron fluxes will also be considered.

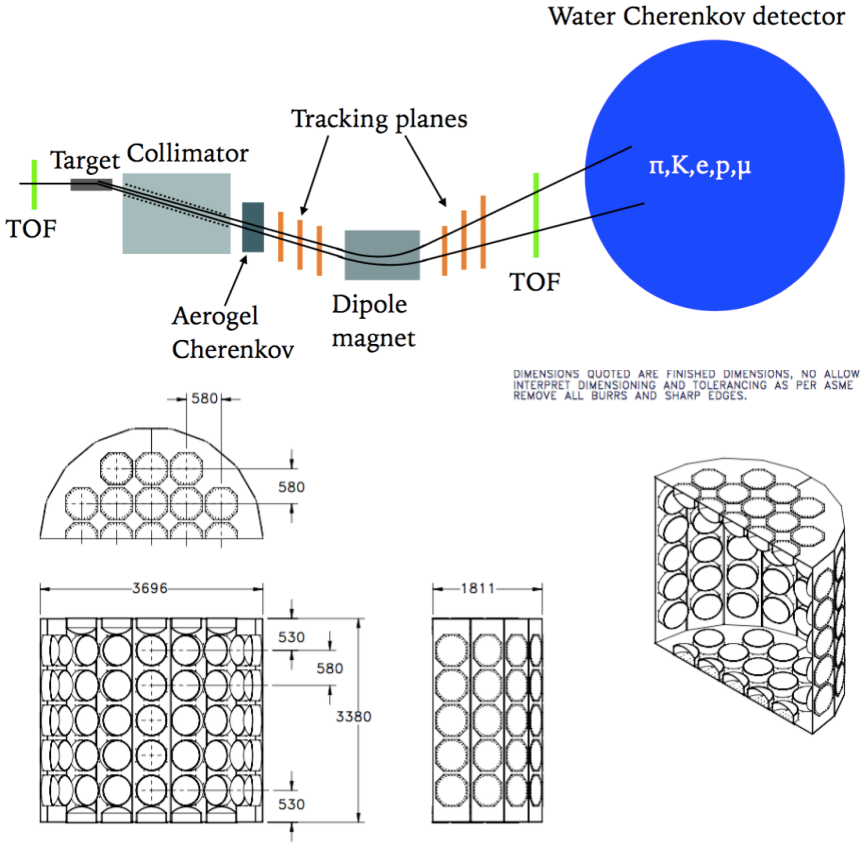

FIG. 3. Top:Conceptual drawing of the WCTE. Bottom: Cross section drawings of the multi-PMT layout inside the detector.

The WCTE will have multiple phases of operation. The first phase will use standard ultra-pure water and the deployment of multi-PMT photosensors and calibration systems that will be used in the IWCD. The goal of this phase is to match as closely as possible to the detector configuration that will be used in the initial phase of the IWCD. Fig. 3 (bottom) shows the arrangement of the multi-PMT photosensors in the detector. For full instrumentation, 132 multi-PMT modules will be installed and operated. The WCTE will allow the performance and calibration of the detector and its components to be evaluated. Fig. 4 shows a sampling of reconstructed quantities for simulated events in the WCTE for particles entering at the center of the upstream side of the tank, as well as particles produced at the center of the IWCD tank. The resolution for reconstructing the vertex, momentum and particle type in the WCTE is similar to the IWCD, indicating that the WCTE is a useful platform to evaluate the performance of detection and calibration systems to be used in the IWCD.

The initial phase of the WCTE will also be used to evaluate important physics processes that are necessary for the accurate modeling of the detector. For example, the production of Cherenkov light at large angles relative to the particle propagation due to delta rays will be measured. The timing resolution of the multi-PMT photosensors, $\sim$ 700 ps RMS, corresponds to a travel distance of 15 cm in the detector, allowing high angle light from delta rays or scattering to be separated from light produced by reflections. The initial phase will also be used to study the properties of pion scattering in the detector, which can produce topologies with more than one Cherenkov ring for each initial charged pion, or rings that are not completely filled in if the pion is absorbed before dropping below the Cherenkov threshold.

The second phase of the experiment will include loading with $Gd_2(SO_4)_3$ to enhance the neutron detection capability of the detector. Super-K and Hyper-K will use measured neutron multiplicities in neutrino interactions to make statistical separation of neutrinos and antineutrinos or exclusive final states in neutrino interactions. Neutron detection will also be used to tag atmospheric neutrino interactions that are backgrounds to nucleon decay searches. To properly model the neutron production and detection, it is necessary to model the production of secondary neutrons as particles traverse

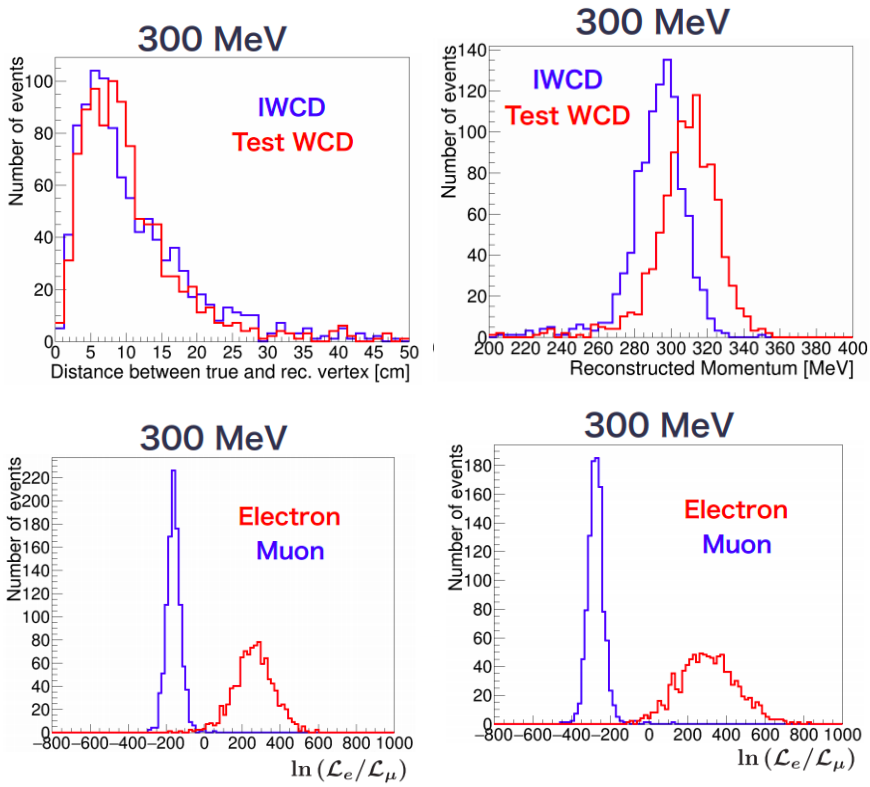

FIG. 4. Top: Vertex resolution (left) and momentum resolution (right) for reconstructed 300 MeV electrons simulated in the the WCTE and IWCD. Bottom: Particle identification distributions for simulated 300 MeV electrons in the WCTE (left) and IWCD (right).

and interact in the detector medium. During this phase, the production of neutrons from particles propagating through the detector will be measured.

Fig. 5 shows the predicted multiplicity of detected neutrons when a primary hadron traverses a generic water Cherenkov detector of sufficient size. Significant production of secondary neutrons is expected and the prediction varies depending on the model. The WCTE with $Gd_2(SO_4)_3$ loading will be able to measure these neutron multiplicities. In addition to the neutron production from hadrons, the neutron production from μ^- capture on O nuclei will be measured. This process is another source of secondary neutron production. These neutrons can provide another source of statistical separation of neutrinos and antineutrinos (μ^- and μ^+) in muon (anti)neutrino charge current interactions.

The third phase of the WCTE will see the deployment of water-based liquid scintillator (WbLS) in the experiment, as well as novel photodetectors designed to enable the separation of Cherenkov and scintillation light. This phase of the experiment will be focused on characterizing light scintillation and Cherenkov light production for various incident particles. Photodetectors that separate Cherenkov and scintillation light by timing or spectrum will be used and their performance will be evaluated. Multiple runs with different scintillator mixes may be carried out during this phase.

III. EXPERIMENTAL APPARATUS

In this section, we provide a brief description of the components of the water Cherenkov test beam experiment, including the detector and beam components.

A. Beam-line, Secondary Target and Spectrometer

As suggested in the previous subsection, the water Cherenkov detector will be placed in a charged particle beam which includes $e^{\pm}$, $\mu^{\pm}$, $\pi^{\pm}$, $K^{\pm}$, and p. The desired momenta are between 140 MeV/c and 1200 MeV/c. The requirement of low momentum pion and muon beams is placing a conflicting constraint on the WCTE. To get low momentum pions in

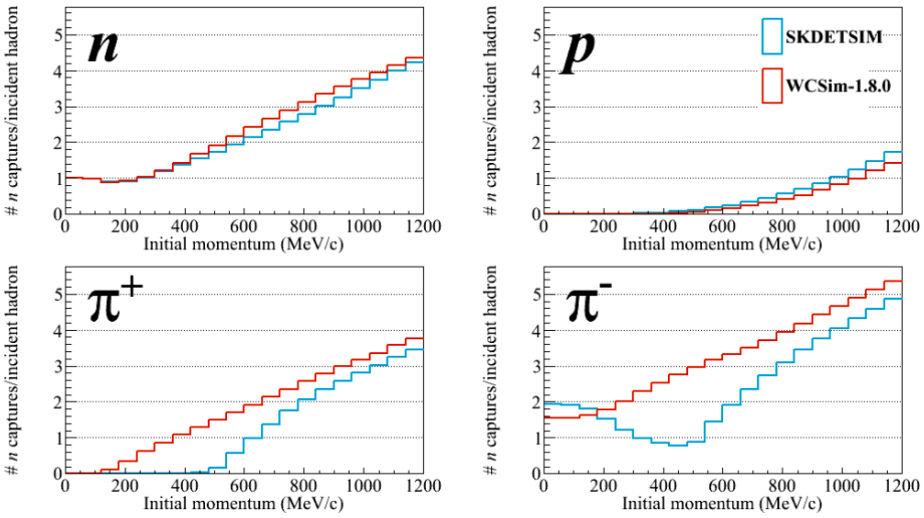

FIG. 5. Detected secondary neutron production multiplicities for neutrons produced by hadrons propagating in a water Cherenkov detector. Simulated with GEANT4-based WCSim and SKDETSIM, the simulation package for Super-K.

the desired energy range, the beam-line must be less than 10 m long. On the other hand, muons are products of pion decays and to achieve low momentum muon beam, the beam-line should be longer to allow most of the pions to decay. Therefore, we need to run the WCTE in two different configurations: a short setup with pion enhanced beam and a long setup with muon enhanced beam.

Two experimental areas at CERN are able to accommodate the Water Cherenkov Detector: North Area and East Area. The North Area receives a 400 GeV/c primary beam from Super Proton Synchrotron (SPS) and provides experiments with secondary electron and hadron beams from 10 GeV/c up to 400 GeV/c. In contrast, the East Area receives a 24 GeV/c primary proton beam from Proton Synchrotron (PS) and generates secondary hadron and electron beams from 0.3 GeV/c and 15 GeV/c. The secondary beam intensity is up to 10^6 and 10^7 particles per spill for East and North Area, respectively. Unfortunately, the minimum beam momentum in North Area is too high for the test experiment. Similarly, the secondary beam-line in the East Area is too long to provide a low momentum pion and kaon beams. However, beam-lines in the East Area can provide a low momentum muon beam.

The spectrometer setup

To generate low momentum hadron beams we propose a secondary target and a compact spectrometer placed several meters upstream from the water tank. A small neodymium dipole purchased by TRIUMF group (see Fig. 6) together with wire chambers can be used for tracking and momentum measurement.

We have developed a Monte Carlo simulation based on GEANT4.10.05.p1 to study the spectrometer performance and to estimate the produced particle rate. All hadronic interactions are simulated with FTFP_BERT physics list. Simulated geometry includes the magnet and eight wire chambers. Chambers are placed in pairs to measure x and y particle positions. Two pairs are located upstream from the magnet and the other two are downstream from the magnet. The distance between the pairs of wire chambers is around 25 cm. The assumed wire pitch is 1 mm which gives position resolution of about 300 μm. The expected momentum resolution has been studied by reconstructing track parameters of low momentum pions passing through the magnet and the tracking layers. The obtained resolution presented in Fig. 7 is satisfactory for the WCTE. However, the resolution can be easily improved if more precise detectors are used or the separation between the wire chambers is increased.

Since the beam will be generated close to the water Cherenkov detector, a choice of the target, beam momenta, and the shielding configuration need to be taken into careful consideration to avoid high background particle rates. In this study, we have used a 30 cm long graphite target and 30 GeV/c proton and pion beams to simulate the typical secondary beam momenta in the North Area. Shorter and denser targets made of lead or tungsten have been considered but discarded because of the high gamma-ray and neutron background rate. The water tank has been placed at 8 m from the target. The beam and the target are angled at 450 mrad with respect to the axis between the target, spectrometer and the water tank. The angle has been chosen so that surviving beam particles miss the magnet and the water Cherenkov

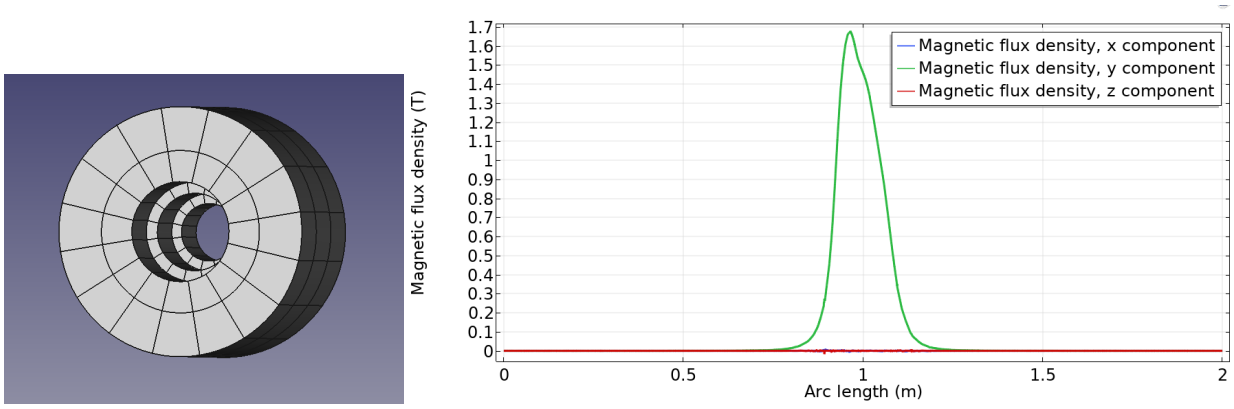

FIG. 6. The neodymium magnet (left) and the magnetic field generated by the magnet obtained from the COMSOL simulation (right). The magnet is consists of three longitudinal layers, each 5 cm thick and with the external diameter equal to 20 cm. The inner diameter changes from 4.6 cm to 8.0 cm. The maximum magnetic field is around 1.7 T with a total bending power of 0.2 Tm.

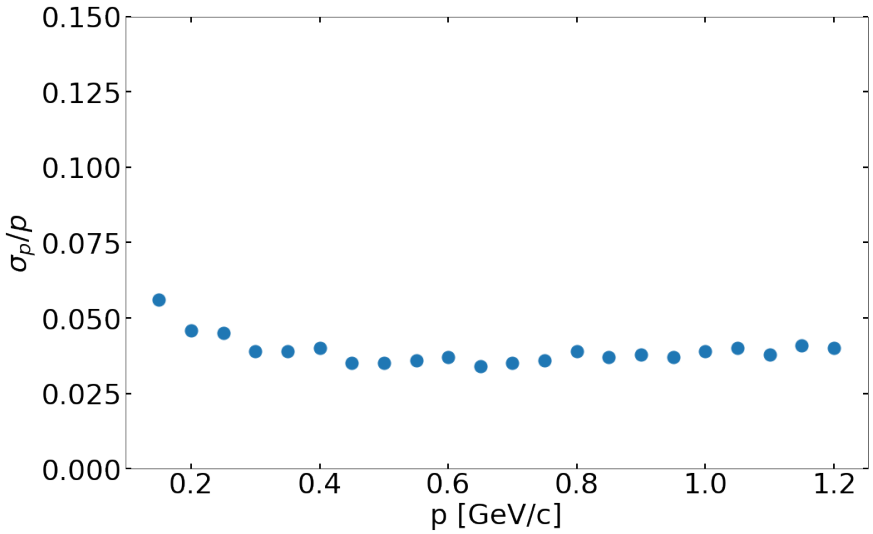

FIG. 7. The momentum resolution.

detector. Concrete shielding has been placed to block most of the produced particles which are not going through the spectrometer, but it allows the surviving beam to pass through. The total thickness of the concrete shielding is 320 cm. Additional 1 m thick water tank is placed on the downstream side of the concrete shielding to block most the low momentum neutrons. The shielding blocks are stacked to create a 80×80 cm^2 opening for particles passing through the spectrometer. The simulation geometry and example event displays are shown in Fig. 8.

The results of the simulation for pion and proton beams are presented in Fig. 9. The background is defined as gamma rays, neutrons, and charged particles not passing through the opening in the shielding. Selected particles are defined as charged particles passing through the magnet, tracking layers, opening in the shielding and hitting the water Cherenkov detector. The background rate is uniform over the cross-section of the detector except in the center and at the edge of the tank closest to the surviving beam. The selected particles are mostly π^+ and p. Fraction of selected particles are summarized in Tab. I. In the current configuration, the rates of negatively charged particles are strongly suppressed. This is a consequence of the magnet orientation and can be easily reversed by rotating the magnet by 180°.

The total background rate is a couple of times higher compared to the rate of the selected particles. However, the fraction of events in which selected particle is accompanied by an additional selected or background particle is around 10%. This is illustrated in Fig. 10. In many cases, the background particle is a neutron. The neutron capture in the water Cherenkov detector can be removed from the signal by timing.

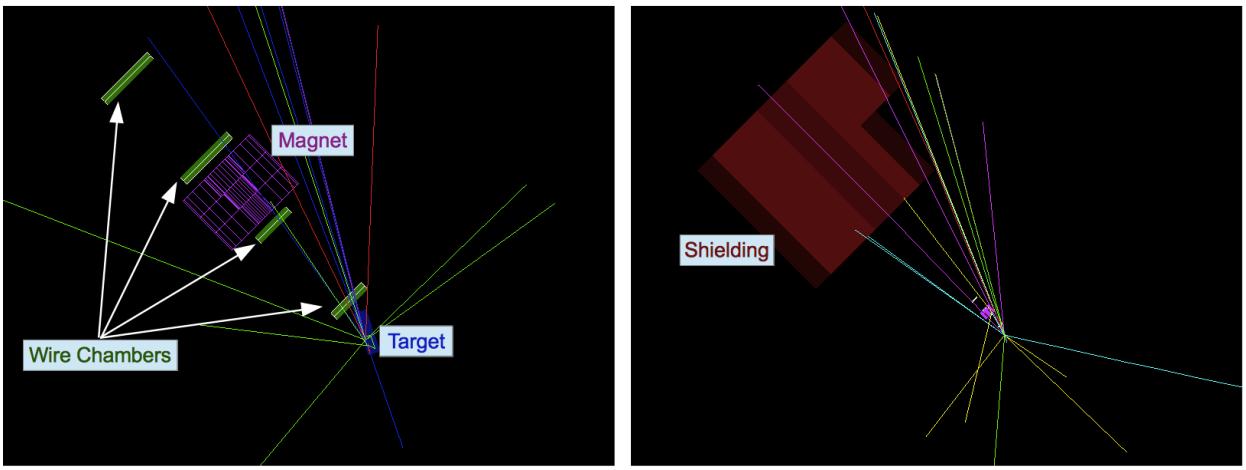

FIG. 8. The beam simulation geometry and an example event zoomed into the spectrometer region (left) and zoomed out to show the shielding (right). The gap in the shielding for the tertiary particles of interest is hidden in this view.

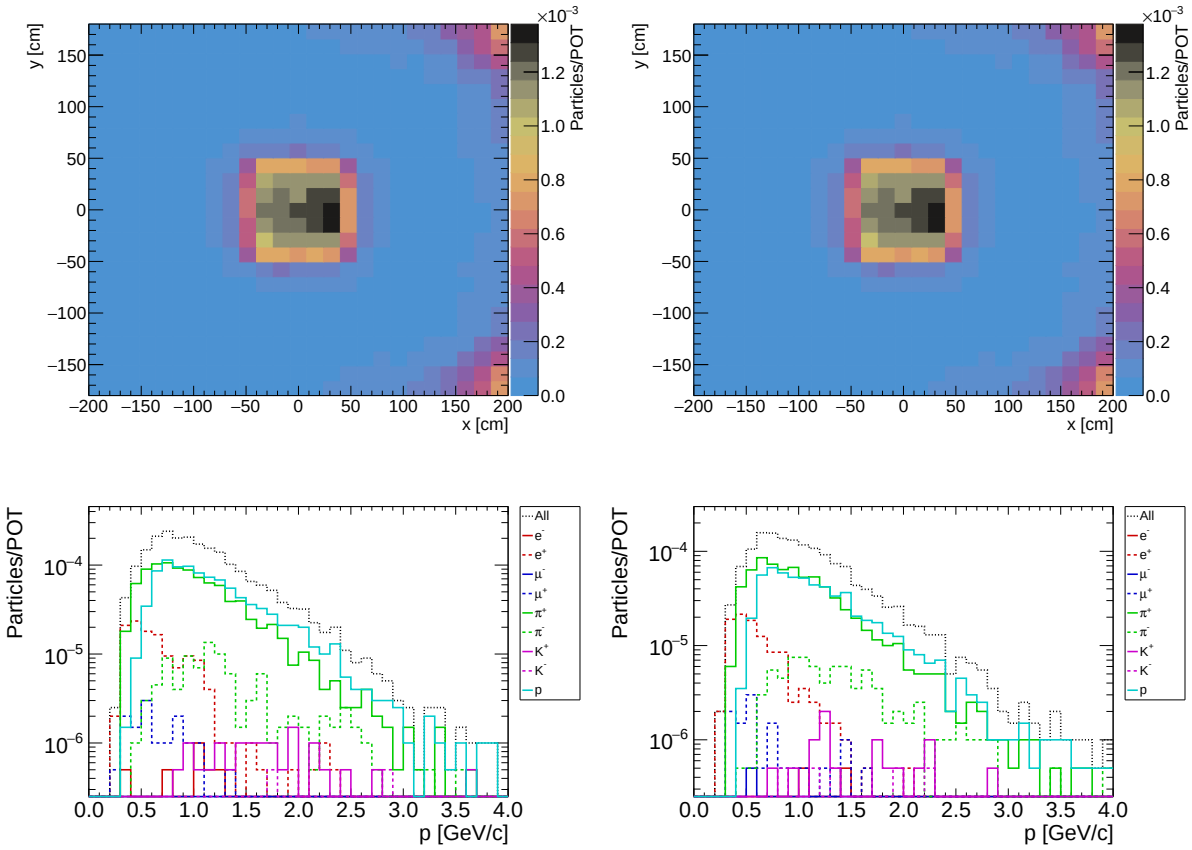

FIG. 9. The selected particle rate hitting the cross-section of the water tank for proton beam (top left) and pion beam (top right). Momentum distribution of selected particles for proton beam (bottom left) and pion beam (bottom right).

TABLE I. Fraction of different selected particles for proton and pion beams.

	Particle fraction [%]								
Beam	e^-	e^+	μ^-	μ^+	π^+	π^-	K^+	K^-	p
p	0.1	5.7	0.0	0.6	43.9	4.3	0.6	0.1	44.7
π^+	0.0	6.9	0.0	0.8	46.6	5.2	0.6	0.2	39.7

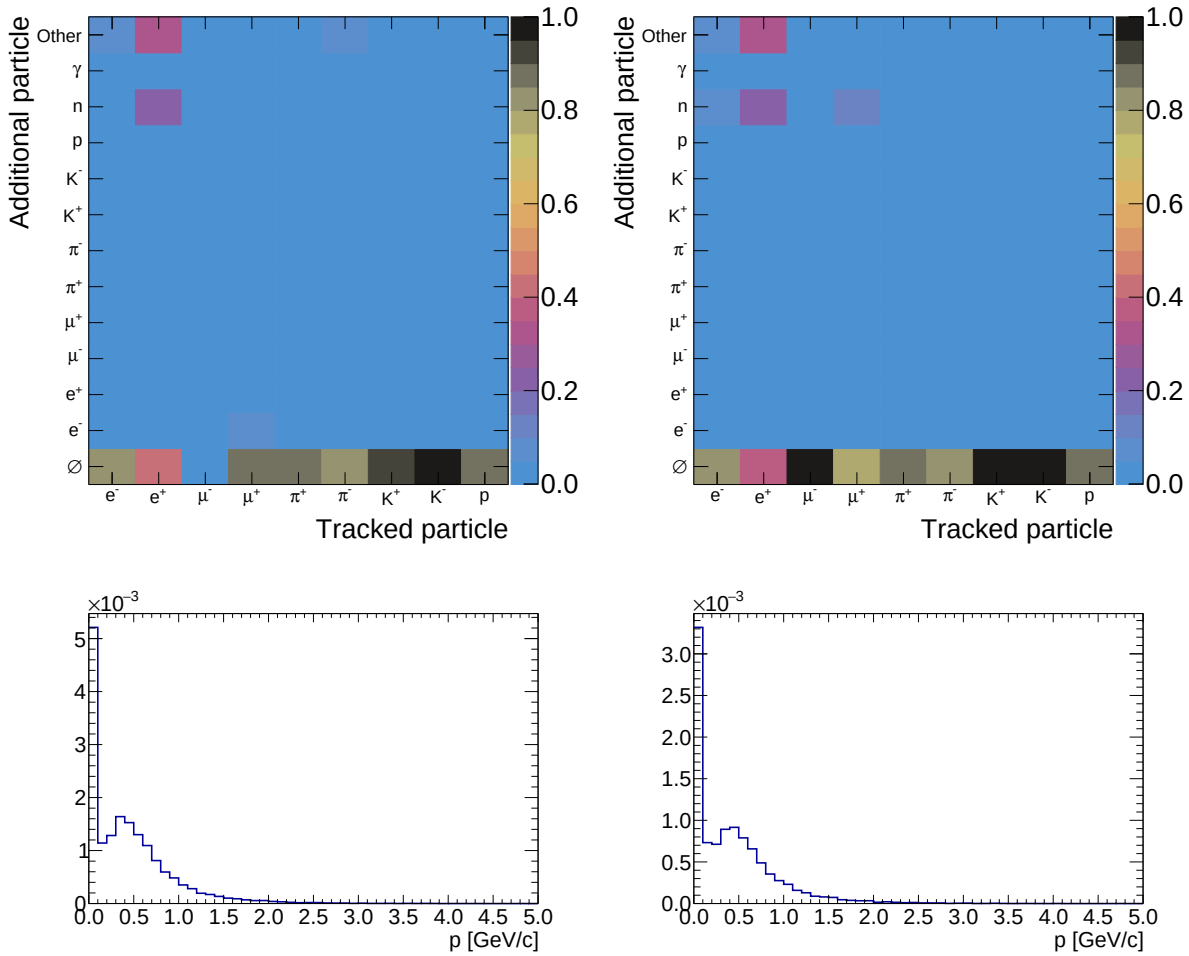

FIG. 10. The fraction of selected particles accompanied by zero or one additional particle for proton beam (top left) and pion beam (top right). The bin "Other" contains events with multiple additional particles. Background neutron momentum distribution for incoming proton beam (bottom left) and pion beam (bottom right).

The momentum distribution of background neutrons is presented at the bottom of Fig. 10. Significant fraction of neutrons have momentum around 500 MeV/c. Therefore, this spectrometer configuration can be used for neutron capture measurements in the water Cherenkov detector. However, measuring neutron momentum will be a challenge, and it is currently being discussed by the collaboration.

The beam rate study presented here is only preliminary and the choice of the secondary target, incoming beam momenta, and the shielding configuration will be decided after discussion with beam experts. However, the results of this study demonstrate that it is possible to achieve low momentum particle rates of $2000 - 3000$ particles per 10^6 incoming beam particles with sufficiently low background rates.

B. multi-PMT Photosensors

Single kiloton scale water Cherenkov detectors such as the IWCD are significantly smaller than Super-K and Hyper-K, and therefore faces different challenges in photon detection. Cherenkov photons will typically travel shorter distances from production to detection and so Cherenkov rings will project onto smaller areas. Using the same 50 cm diameter PMTs as Hyper-K would result in poor event reconstruction, especially for multi-ring events and events near the detector wall. These smaller detectors require a finer spatial granularity in order to achieve equivalent sampling. The detector size also necessitates improved timing resolution in order to improve vertex resolution. This is important for defining the fiducial volume and rejecting backgrounds from interactions in material outside the fiducial volume. The photosensors are required to have a transit time spread of ~ 1 ns, which corresponds to a ~ 20 cm light propagation distance.

In order to satisfy these requirements the Hyper-K IWCD will be populated with multi-PMT (mPMT) optical modules, an array of 19 smaller 8 cm diameter PMTs. The mPMT photodetector design is inspired by the spherical modules developed for the KM3NeT experiment [5]. However, the IWCD photosensors will be largely forward facing since they instrument and surround the region of interest inside the detector. Some radius of curvature for the PMT array will be retained so that the individual photosensors have different orientations and image different parts of the detector. This provides directional information about the detected photons which will improve vertex reconstruction. A further benefit to this modular approach is realized in the cabling and waterproofing of the photosensors. An increase in the number of PMTs would typically increase the amount of cabling and waterproofing. Housing many PMTs in a single vessel along with the readout electronics reduces the amount of cabling necessary. Waterproofing and pressure protection are provided by a single vessel for all 19 PMTs housed in the mPMT.

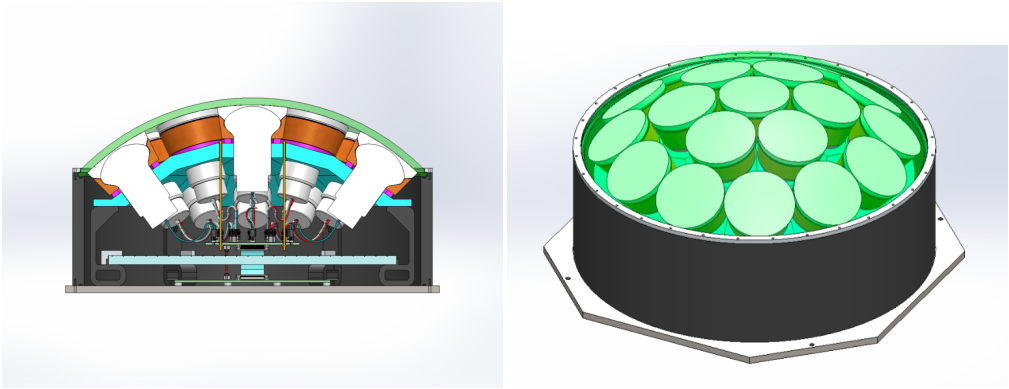

FIG. 11. Left: The cross section view of the mPMT module with 19 8 cm diameter inward-facing PMTs, and integrated front-end electronics. Right: The external view of the mPMT module.

The design of the mPMT module can be seen in Figure 11. An array of 19 8 cm diameter PMTs is supported by a hemispherical 3D printed support matrix. The PMTs are housed in 3D printed cups which interface with the matrix to fix the orientations of the PMTs. A layer of Poron between the matrix and the cup absorbs compression of the acrylic dome under pressure. The PMTs are optically coupled to the acrylic dome by a silicon gel. Wacker ELASTOSIL RT 604 A/B was chosen because of its optical properties, compressibility, and non-tacky surface. EVONIK UV transmitting PLEXIGLAS GS was chosen for the acrylic dome, which has high transmittance and low levels of Radon emission. Reflector cones are surround each PMT to increase the photocoverage by approximately 30%. A scintillator panel is placed inside the mPMT, improving the efficiency to detect backgrounds arising from interactions in the mPMT material or outside of the detector.

The module is housed in a 50 cm diameter and 16 cm length cylinder closed by a stainless steel plate at the base and an acrylic dome at the top. For the WCTE, the cylinder will be made of PVC, however alternative plastic options are being investigated for the IWCD. In the future, improved versions of the mPMT might be considered for use in Hyper-K.

The WCTE will be instrumented with 132 mPMT modules. mPMT design optimization and performance tests are currently underway. A prototype is shown in Fig. 12. Production of the mPMTs for the WCTE will begin in 2020.

FIG. 12. Top (left) and side (right) views of the mPMT prototype.

C. multi-PMT Electronics

Two essential electronic components of the mPMT module are the high voltage supply and digitization electronics. The former ensures that each PMT gets the correct voltages to produce a signal in response to incoming photons. The considered options involve both the 'cathode grounded' scheme with anode at positive high voltage and the 'anode grounded' scheme, with the cathode at negative high voltage. Each has its benefits - the former (and preferable) option provides for a lower overall dark rate, while the latter allows for DC coupling. To cope with the limited budget for power consumption, we cannot use a standard HV supply and a resistive voltage divider. Instead, we have developed an active power supply based on the Cockcroft-Walton voltage multiplier, with PMT dynodes connected to individual taps of the multiplier chain. It is a similar solution to the one adopted in the KM3NeT PMT base design. Revised HV board prototypes have been built and tested. Power consumption of 12.5 mW per channel has been achieved, corresponding to a 237.5 mW of total power consumption for all the HV boards within the mPMT module.

The selected digitization approach for IWCD, as well as the WCTE, is based on full waveform sampling using the FADC. The reason is that having access to the waveform provides more information for complicated pulses, and it does not introduce dead time. Both of the above are particularly beneficial for the IWCD and WCTE mPMTs, where it is expected that there will be substantial signal rates within the different bunches of the beam spill.

The FADC digitization option for the mPMT electronics is shown in Figure 13. The PMT signals are transformed into differential signals using a transformer and are then transmitted to the mainboard via a twisted pair flat cable. The same cable is used to transmit HV and slow control signals as well as the power for the PMT base. The differential signals reaching the mainboard are shaped to meet the Nyquist sampling criterion and are then digitized by a 125 MSPS 12-bit FADC. The ADC data is transferred to an FPGA, where digital signal processing (DSP) techniques are used to find pulses and calculate their charge and time arrival. The processed information on each hit is sent from the front-end electronics within the mPMT module to the concentrator card via an ethernet cable. For more complicated pulses, and diagnostic purposes, the raw ADC samples can also be saved. The main electronics board sits on top of a stainless steel base plate which acts as a radiator.

Each mPMT has a single waterproof cat-5e cable that provides power, clock, sync signals, and a network connection. We expect to have an mPMT Concentrator Card (MCC - Fig. 14) which connects to 24 different mPMTs and provides power, clock and sync signals and communication with the downstream DAQ system. Given the geometry of the WCTE, the MCC will probably be outside the tank. While distributing the clock, sync, and power to the mPMTs should be fairly straightforward, the collection and routing of the data packets from the mPMTs through the MCC will be more complicated. There are a couple of options for the data transfer between the mPMT and MCC, which are being actively evaluated. Those include using an Ethernet standard over two pairs (100 Mbit link), replacing the Ethernet physical layer with LVDS link but keeping the protocol part or using custom protocol. The latter - while more time consuming to develop has an advantage of more freedom in choosing the speed of the link as well as encoding clock along with the data, which may allow for two redundant links in a single Cat 5e cable.

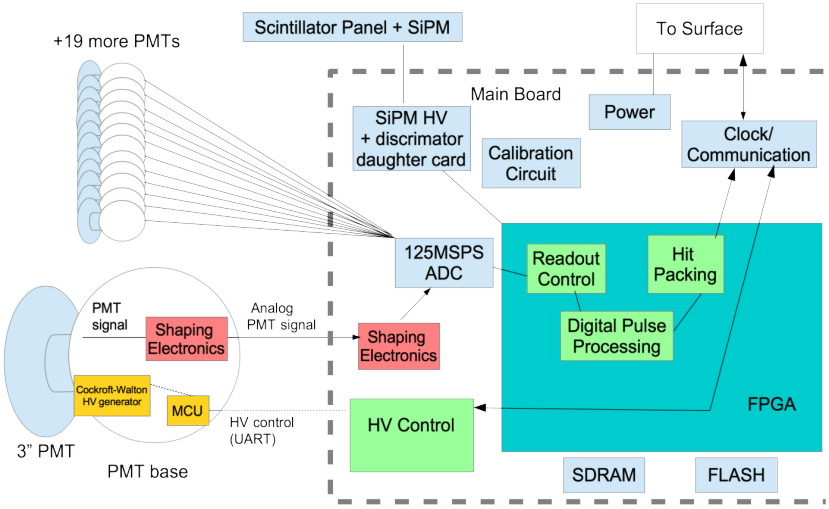

FIG. 13. Block diagram of the mPMT mainboard for the FADC digitization option. The PMT signal is shaped with circuits on the PMT base and mainboard, then digitized with 125 Msps ADC. ADC samples are processed in an FPGA to find pulses and extract the pulse parameters.

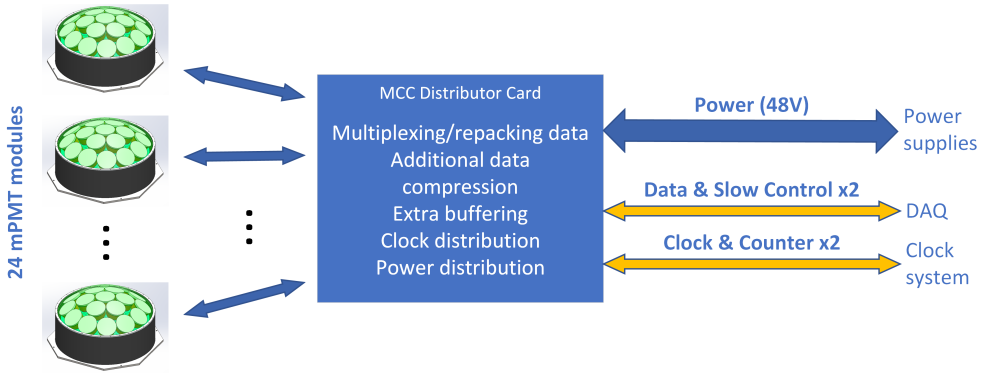

FIG. 14. Connections of multi-PMT to the DAQ with the Multi-PMT Concentrator Card (MCC). The MCC is responsible for distributing clock and power to the mPMT modules and for collecting data from the mPMT modules and sending it to the downstream DAQ system via an optical fiber link.

D. Data Acquisition Systems

The Data Acquisition systems for the proposed IWCD and WCTE will make use of the ToolDAQ framework. ToolDAQ is a modular and scalable DAQ software system that is planned for deployment in Hyper-K and is also being used currently by other experiments.

The 2 x 1 Gbps optical data connections from the MCCs will be connected into two different commercial network switches. This will allow redundancy and the connections will operate as an active backup bonded pair transferring TCP/IP packets to the Layer 3 switches. From here two Readout Buffer Units (RBUs) made from commercial server hardware will also be connected to both of these switches via 2 X 10 Gbps optical links to each switch. The RBUs wll used to buffer and catalogue the hits that are streamed to them from the MCCs. This system can be expanded or reduced depending on the number of MPMTs and MCCs deployed in either the WCTE or IWCD tank and the level of redundancy required. A separate triggering and event building server (TPU/EBU) (with a possible redundant clone) will then be connected to the RBUs to make triggering decisions based on the number of hits seen in the detector over a sliding window and external triggers from beam line or calibration sources. Once a positive trigger decision is made this server will then build and write an event to raided storage installed within it. This configuration can be seen in Figure.15. Event data can then be transferred off site for longer term storage.

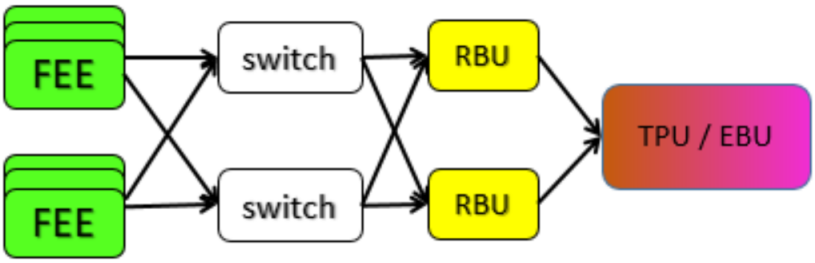

FIG. 15. DAQ schematic for the WCTE and the IWCD. The schematic shows network connections between the front end electronics/ multi PMT concentration cards (FEE), the readout bufer units (RBU) and the triggering processing and event building server units (TPU/EBU)

E. Slow Control and Monitoring

Slow control and monitoring of the electronics and DAQ will take place via ToolDAQ and be displayed with user interfaces via web pages that will be hosted on either a separate server installed in the experiment hall or the triggering and buffering servers depending on server specs and loading. From here voltages, temperatures, trigger rates, run start and stop controls, as well as many monitoring plots of merit will be controlled and commands sent through the DAQ network described above to the relevant MCCs (and on to the MPMTs) or triggering and build servers. Data and run information will also stored in an mirrored SQL servers that will log run configurations start and stop times and other useful information.

F. Calibration Systems

The proposed IWCD and WCTE calibration systems are based on the Super-K calibrations [6], with appropriate modifications. These include diffuse and collimated light sources mounted on the tank wall and deployment of a laser diffuser ball, NiCf source, and potentially an AmBe source. Special consideration is required for the smaller scale of the IWCD, such as smaller/older radioactive sources so as not to saturate the detector. The fiducial volume is relatively small compared to the full detector volume, imposing stringent requirements on the vertex reconstruction. Characterizing the detection efficiency also becomes a challenge as most of the active volume is near the edge of the detector, where the efficiencies of event reconstruction and particle identification vary rapidly over relatively small distances. Finally, to maximize the use of resources, the calibration systems should be designed with consideration of installing on the movable IWCD.

There are examples of water Cherenkov detectors similar to the IWCD in size ($\sim$1 kiloton), such as Kamiokande, IMB, the K2K 1 kiloton detector, and SNO. Their systematic errors on efficiency are several % or more, which are significantly larger than what is required for IWCD (1-2%). This is one of the most challenging aspects of IWCD and a critical point for the success of the Hyper-K project. The SNO experiment did the most precise measurement among the small water Cherenkov experiments by controlling their efficiency error to the limit of uncertainties in the angular responses of PMTs and the positions of each PMT in the vessel, which are tightly related.

Thus, in addition to the calibration sources similar to Super-K, the IWCD will attempt geometrical calibration by photogrammetry and ex-situ calibrations of PMT angular response at photosensor test facilities (PTFs). In order to calibrate physics processes, such as the response to hadron interactions and light scattering in the detector, a test beam of known particle types and momenta is required.

The WCTE will establish state-of-the-art calibration systems and procedures for small water Cherenkov detectors and provide the necessary physics measurements to understand the production of Cherenkov light by charged particles in water.

Calibration sources and deployment system

The deployment system considered for the IWCD and WCTE is a manipulator arm deployed from the top of the tank. The system is similar to the ones used by KamLand, a manipulated bar, or a manipulated source like Daya Bay and SNO. The former has an advantage of providing a well defined scale between multiple source positions while the latter are technically simpler. The deployment system will position the diffuser ball at various positions in the detector. It will

also deploy a 360 camera for photogrammetry, as discussed below. There will be fixed LED and laser light sources, currently developed for Hyper-K and testing in Super-K, on the tank walls to provide both focused and diffuse light.

Geometrical calibration using photogrammetry

An incomplete understanding of the *in-situ* photosensor position limits the precision of the final event reconstruction. Sensor position uncertainties arise from the support frame shifting due to sensor buoyancy and water pressure. This displacement was as large as several cm for SNO, and the distortion of the tank was apparent by eye in the case of the K2K 1 kiloton detector. SNO+ developed a new technique of measuring the PMT positions using photogrammetry [7]. Photogrammetry will pinpoint the position of each sensor by deploying underwater cameras, taking multiple photographs of the detector, and performing stereoscopic reconstruction.

For the WCTE, we will affix two to four $\sim$ 40M pixel mirrorless digital cameras in underwater housings to the mPMT support structure. An additional $\sim$120M pixel and/or 360 camera will be deployed with the source deployment system, providing pictures of the detector at various positions and angles. By fitting the images, a 3D image of the inner surface of the detector can be reconstructed that will be millimetre level precision.

Ex-situ calibration of photosensor angular response

The angular response of each photosensor can be a significant source of systematic uncertainty, in particular when it is coupled with displacement of the photosensors. Photosensor test facilities (PTFs), like the one currently operating at TRIUMF, can illuminate the surface of a PMT at a specified angle and position using a laser-equipped motorized gantry. A second gantry can be used for characterizing reflections from the PMT surface or other detector materials. The PTFs will provide detailed maps of the angular and position response and reflectivity of the multi-PMTs used in the WCTE.

Natural Particle Sources

Additional particle sources arise from cosmic muons and the Michel electrons from those that stop in the detector. A summary of the energy scale calibration obtained from these sources in Super-K is shown in Figure 16, including the difference from MC of the means of the Michel spectrum, muon momentum/range distributions, and neutral pion mass. The imperfect agreement at the $\sim 2\%$ level enters as a systematic error and limit the precision of high level neutrino oscillation analyses.

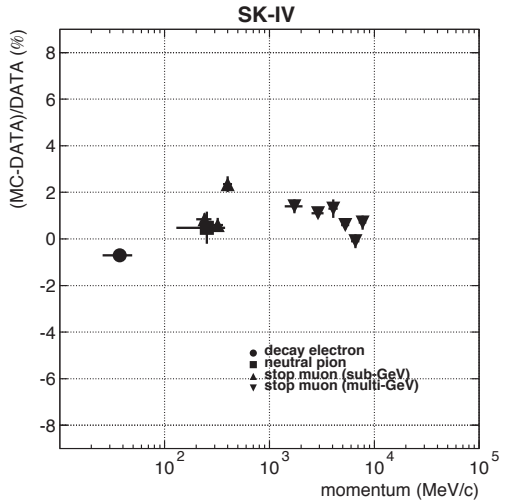

FIG. 16. Measurements of the absolute energy scale in Super-K compared to MC with various high energy particle sources.

In order to improve this and achieve a 1% level total systematic error, a detailed understanding of the detector must be established using fundamental physics parameters such as water scattering and absorption, material reflectivities, PMT time and charge responses, detector geometry, and so on. This model should be able to describe every calibration source and data set such that any data/MC discrepancies can be understood via reasonable tuning of parameters. Then, a charged particle beam will provide a sample of particles with known energies that span the range of interest for IWCD and Hyper-K, that can help understand the systematic discrepancies in e.g. Figure 16. Furthermore, the WCTE will provide essential data by filling in the gaps where natural particle sources cannot probe.

TABLE II. Non-exhaustive list of fundamental physics parameters that affect and thus can be constrained by, to first order, the various calibration sources and measurements.

Systematic Parameter	Light Injectors, Diffuser Ball	Radioactive and Particle Sources	PMT Test Facilities	Photo-grammetry	CERN Beam
Geometry	✓	✓		✓	
Water	✓	✓			
Reflections	✓	✓	✓		
Timing	✓	✓			
PMT Response	✓	✓	✓		
Cherenkov Physics		✓			✓

Table II summarizes the calibration sources and measurements described above, together with the known fundamental parameters affecting such measurements. Ideally, one could design calibration sources or measurements that diagonalize this matrix, however, in-situ measurements necessarily convolute most of the parameters and suffer from several degeneracies. Ex-situ measurements, such as the PTFs, or photogrammetry help to disentangle some parameters, but several independent light and particle sources will be needed to fully constrain the problem for a robust and precise measurement of the Cherenkov physics with the test beam.

G. Dichroicon Wavelength-Separating Cones

When using Water-based Liquid Scintillator (WbLS), the ability to separate Cherenkov and scintillation light can substantially enhance the information extracted from each light source. One method for separating these light sources at the hardware level is the Dichroicon, which is a Dichroic Winston cone that reflects the longer-wavelength portion of the Cherenkov spectrum toward a central red-sensitive photodetector, and allows the shorter-wavelength scintillation light to pass through the cone to a blue-sensitive photonsensor, and shown in Figure 17.

The wavelength distributions of Cherenkov light, PPO, and PTP are shown in Figure 17. By using a Winston cone with a dichroic filter at 450 nm, only the long-wavelength portion of the Cherenkov spectrum is directed toward a central PMT region that accepts wavelengths above 450 nm, which then provides a high-purity measurement of the direction-sensitive Cherenkov light signal. The light that passes through the Winston cone constains nearly all of the scintillation light, as well as the low-wavelength portion of the Cherenkov light, such that nearly all of the photons are still collected to preserve energy resolution for low-energy signals.

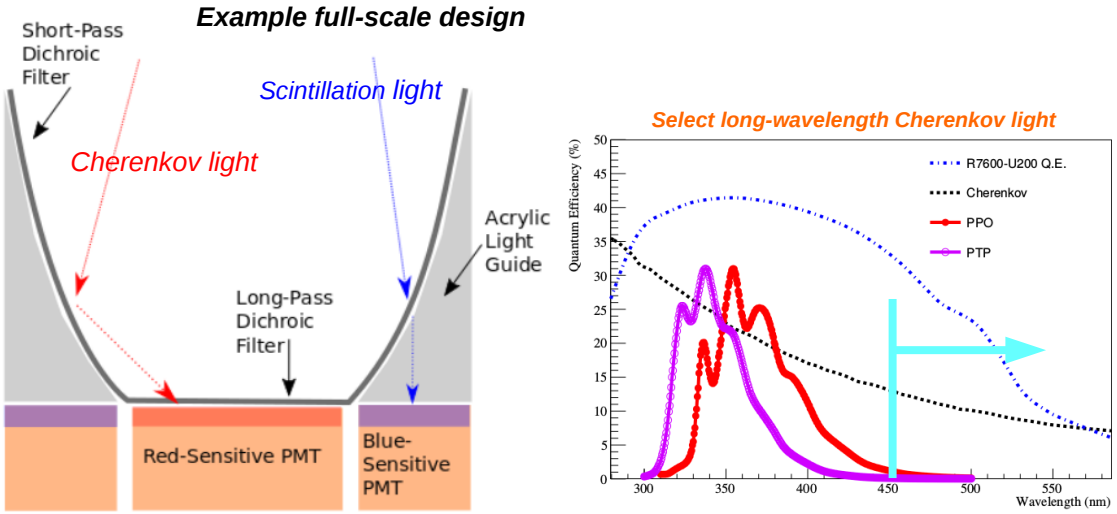

FIG. 17. The left figure shows a schematic of the Dichroicon, and the right figure shows the wavelength distribution of Cherenkov light, POP, and PTP.

Several dichroicons can be deployed in the WCTE to study the separation and collection properties of these devices. Many of the performance metrics can be determined in the pure water phase of the experiment, since Cherenkov photons

will be found in high- and low-wavelength sensitive regions. Additional studies in the WbLS phase are needed to study the efficiency for excluding scintillation light in the central Cherenkov-sensitive region.

H. Water System

Super-Kamiokande has a diagonal dimension of ~ 50 m and an attenuation length for visible photons of ~ 100 m. To ensure that the fractional attenuation of photons in the WCTE is equivalent to or less than in Super-K, an attenuation length of ~ 11 m or better should be achieved in the WCTE. Super-K achieves ultra-pure water with a system that includes microfiltration filters, degasifiers (vacuum and/or membrane type), reverse osmosis membranes, deionization resins, and exposure to intense ultraviolet light. The water flow rate in Super-K is $\sim$60 ton/hr. The WCTE ultra-pure water system may be a scaled-down version of the Super-K system. To ensure that sufficient attenuation length can be reached quickly after filling with water or changing the water conditions, a maximum circulation rate of > 500 liters/hr should be achieved. Commercially available water systems can meet these requirements and may be used for the WCTE.

Operation with $Gd_2(SO_4)_3$ or WbLS will require modifications to the water system. In the case of $Gd_2(SO_4)_3$, a molecular band-pass filter system is used to remove impurities while keeping the dissolved Gd in the water. This system should be added to the water system for the Gd operation mode. Alternatively, given the reduced attenuation length requirements for the WCTE, it may be possible to operate with Gd simply by removing the deionization resins that remove the Gd. In this scenario, the water system would be operated in pure water mode until the desired attenuation length is reached, after which the deionization resins will be removed and the $Gd_2(SO_4)_3$ added to the detector. The removal of $Gd_2(SO_4)_3$ after the Gd phase is complete requires the use of deionization resins.

I. Tank and Support Structure

To maintain material compatibility with ultra-pure water and Gd-loaded water, stainless steel 304 will be used for construction of the tank and support structure for the photosensors. Given the dimensions of ~ 4 m diameter and ~ 4 m height, a commercially available tank can be used for the experiment. The tank lid will be custom designed and produced to accommodate the necessary ports for cabling, calibration source deployment and water circulation. The support structure will be based on the design that is under development for the IWCD. The support structure may be assembled outside of the tank and lowered into the tank, or assembled inside the tank. The photosensors will be installed inside the tank after the assembly of the support structure.

IV. EXPERIMENT RUN PLAN

As discussed in previous sections, we plan to run the WCTE with three different detector configurations: filled with ultra pure water and instrumented exclusively with mPMTs, loaded with Gd and instrumented exclusively with mPMTs, and filled with WbLS and instrumented with a combination of mPMTs and new advanced photosensors. Here we make preliminary estimates of the run time necessary for each phase based on the simulations from Section III A. The beam configuration simulated in Section III A produces $\sim$20 tertiary positron events per 10^6 secondary particles per 100 MeV/c of tertiary momentum. We aim to study a number of reconstructed quantities, including particle misidentification rates as low as 0.1%. To achieve a 3% error on the measured misidentification rates, it is necessary to accumulate at least 50,000 spills if the secondary rate is 10^6. At 2 spills per minute, this corresponds to about 20 days of operation. We expect we will need at least 3 beam configurations to achieve the necessary flux at both low energy and high energy, and for muons. We also assume at least one repetition of the measurements to test changes to the detector configuration. In all, this corresponds to ~ 120 days of operation for each detector phase.

It is expected that the Gd loading and WbLS phases will accumulate similar statistics to the ultra pure water phase. This indicates that the full measurement program of the WCTE will require at least 1 year of beam time, assuming 10^6 secondary particles per spill. This beam time may be reduced if the beam configuration can be optimized to produce larger tertiary fluxes of the particles of interest. This beam optimization study will be a priority for the preparation of the proposal, and we ask for support from CERN beam line experts for the North and East areas in preparing these studies.

V. SCHEDULE

The schedule for the WCTE depends on the realization of the detector and tertiary beam components, as well as the availability of test beam lines and experimental areas at CERN. Completing the design and production of the mPMT photodetectors is likely to drive the schedule for this experiment. A prototype effort is currently ongoing and is expected

to produce prototype mPMTs by the end of the 2019 calendar year. We expect that production of the mPMTs can begin in late calendar year 2020. Hence, we aim for installation of the WCTE from early 2021 and operation from late 2021.

[1] K. Abe *et al.*, "Hyper-Kamiokande Design Report," 2018.
[2] S. Bhadra *et al.*, "Proposal for the NuPRISM Experiment in the J-PARC Neutrino Beamline," 2015.
[3] E. Baussan *et al.*, "A very intense neutrino super beam experiment for leptonic CP violation discovery based on the European spallation source linac," *Nucl. Phys.*, vol. B885, pp. 127–149, 2014.
[4] M. Dracos, "The European Spallation Source Neutrino Super Beam Design Study," p. TUPML068, 2018. [J. Phys. Conf. Ser.1067,no.4,042001(2018)].
[5] S. Adrián-Martínez *et al.*, "Letter of intent for KM3net 2.0," *Journal of Physics G: Nuclear and Particle Physics*, vol. 43, p. 084001, jun 2016.
[6] K. Abe *et al.*, "Calibration of the Super-Kamiokande Detector," *Nucl. Instrum. Meth.*, vol. A737, pp. 253–272, 2014.
[7] Z. Petriw, *An Underwater Six-Camera Array for Monitoring and Position Measurements in SNO+*. PhD thesis, University of Alberta, 2012.